2. Palmer Station (07/01/18 – 03/29/19)

This sections describes quality control of solar data recorded at Palmer Station between 07/01/18 and 03/29/19. This period resulted in a total of 15,698 solar scans, which were assigned to Volume 28. There was a site visit at the end of the reporting period. With the following exceptions, the system operated normally and there are only very few data gaps (Section 2.4):

- The internal lamp was unstable during nine "response" scans. It is not clear whether the cause of this instability was the lamp itself or a poor connection between the lamp's posts and its socket. Affected response scans were not used for processing of solar data and the problem has no impact on the quality of solar measurements.
- The fuse of the device that cools the system's photomultiplier tube (PMT) blew on 2/9/19 and was replaced on 2/11/19. During this period, the noise level of the system was slightly increased and the overall sensitivity of the system was about 12% smaller than typically. As the change in sensitivity is tracked with daily response scan, the effect of the low sensitivity was corrected. However, several solar scans had to be removed from the dataset because of this problem.
- The system's monochromator lost its wavelength position on several occasions after manually executed scans. Typically, the problem was corrected promptly without significant loss of data. However, there are no data for 10/23/18, and 12/12/18 – 12/17/18 because of this problem.

The system's PSP radiometer was unit 27198F3 and had a calibration factor of 8.517 $\times10^{-6}$ V/(W m^{-2}). The radiometer was replaced during the site visit.

2.1. Irradiance Calibration

<u>On-site standards</u>
The on-site irradiance standards for the reporting period were the lamps 200W007, M700, M765, 200WN009, and 200WN010. Lamps 200WN009, and 200WN010 are "long-term" standards, which were left at Palmer Station during the March 2014 site visit. It is the intent to run lamp 200WN009 once per year to compare with the other on-site standards. 200WN010 is run every other year during site visits when all on-site lamps and the traveling standard are compared with each other. Both long-term standards were run during the site visit in March 2019, and the comparison with the other lamps is discussed below.

The long-term standards 200WN009 and 200WN010 were calibrated on 12/20/2013 against lamps 200WN001 and 200WN002 using the same procedure as applied to the traveling standard 200WN014 (see below).

The "working standards" 200W007, M700, M765 had not been calibrated for several years and the comparison with the long-term standards and the traveling standard 200WN014 (see below) indicated that the scales of the lamps have changed by 1-2%. Consequently, the lamps were recalibrated against the traveling standard using absolute scans taken at the start of the site visit. Please see previous Operations Reports for the calibrations history of the three working standards.

<u>Traveling standard traceability</u>
The traveling standard used during the site visit was lamp 200WN014. The lamp had originally been calibrated on 1/13/16 by NOAA/CUCF against lamps 200WN001 and 200WN002. Lamps 200WN001 and 200WN002 had in turn been calibrated by Biospherical Instruments in November 2012 against the NIST standard F-616 using a multi-filter transfer radiometer. NIST standard F-616 is traceable to the detector-based scale of irradiance established by NIST in 2000. At the time lamps 200WN001 and 200WN002 were calibrated, they were also compared with the long-term traveling standard 200W017 of the NSF UV monitoring network. The irradiance scales of NIST standard F-616 and lamp 200W017 agreed to within

0.3%. It can therefore be assumed that the change from 200W017 to F-616 as the primary reference for calibrating the SUV-100 instrument at Palmer Station did not result in a significant step-change. The traveling standard 200WN014 was recalibrated by CUCF against lamp 200WN002 on 7/3/19. The new scale of the spectral irradiance agrees to within ±0.2% (±1σ) with the original scale, established on 1/13/16, confirming that the brightness of the lamp remains essentially unchanged. The newer scale was used for the recalibration of the working standards discussed above.

Figure 1 shows a comparison of all lamps performed on 3/25/19, at the start of the site visit. The scales of spectral irradiance of all lamps agree to within ±0.6%.

Lamps 200W007, M700, and M765 were also compared with each other on 7/2/18, 9/24/18, and 12/17/18. The scales of the three lamps agreed to within ±0.7% on all three occasions.

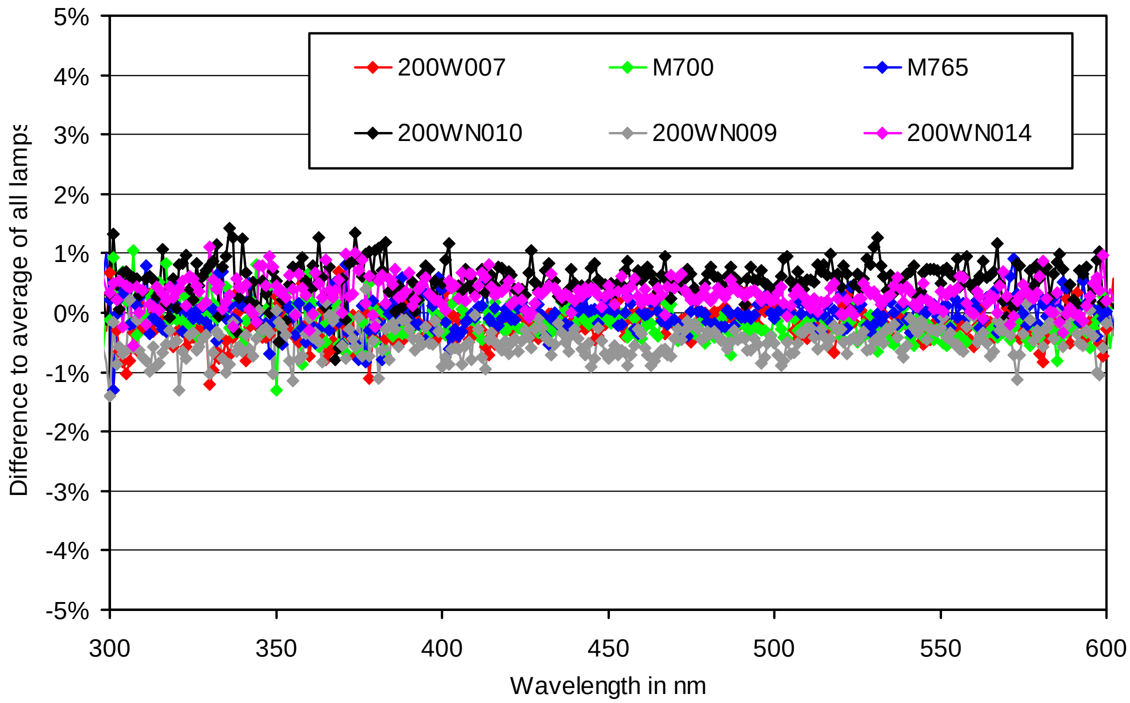

Figure 1. *Comparison of the calibration of on-site standards 200W007, M700, and M765 with long-term standards 200WN009 and 200WN010, and the traveling standard 200WN014 on 3/25/2019.*

To confirm the irradiance scale of solar measurements of the SUV-100 spectroradiometer chosen for the reporting period, the GUV-511 radiometer that is collocated with the SUV was vicariously calibrated against SUV measurements. Calibration factors calculated with this method were compared with similar factors established during previous years. The analysis showed that calibration factors for the GUV 305, 340, 380, and PAR channels that were calculated for the period 2013 – 2019 are in agreement to within ±1.5% (±2σ). The change for the GUV channel at 320 nm is larger because of a known drift of this channel. This result confirms the excellent consistency of SUV calibrations over time.

2.2. Instrument Stability

The radiometric stability of the SUV-100 spectroradiometer was monitored with calibrations utilizing the on-site irradiance standards, with daily "response" scans of the internal lamp, by comparison with measurements of the collocated GUV-511 multifilter radiometer, and by comparisons with results of a radiative transfer model (part of "Version 2" data).

Figure 2 shows changes in TSI readings and PMT currents at 300 and 400 nm, derived from response scans performed between 7/1/18 and 3/29/19. TSI measurements decreased by about 4.0% during this period, indicating that the response lamp became darker by this amount. PMT currents also decrease, however, PMT data are affected by several step changes that are not seen in the TSI data.

- Between 10/22/18 and 10/23/18, the PMT signals abruptly decreased by about 3%. This step change occurred when the system's monochromator lost its wavelength position following an absolute scan. Over the following day, the system was scanning over a different wavelength range than usual. After the wavelength registration was restored, the system's sensitivity was lower, suggesting a change in the monochromator's throughput. The calibration was adjusted accordingly and solar data are therefore not affected.

- On 2/9/19, PMT currents dropped by about 12% when the fuse of the device that cools the PMT blew. The fuse was replaced on 2/11/19. However PMT currents measured after 2/11/19 remained lower relative to those recorded before the failure of the fuse. This suggests that the PMT temperature was not as low as initially. Inspection of the system during the site visit revealed that the fan of the PMT cooler fan was not working properly and was successively replaced. The malfunction of the fan likely caused the fuse to blow and also explains the larger PMT temperature observed after the fuse was replaced. The effect on solar data is minimal as "pairing" with the daily response scans corrects for changes in system responsivity.

- Eleven response scans of the reporting period resulting in low TSI and PMT readings. The problem was most obvious in September and October 2018 (indicated by the ellipse in Fig. 2). The problem could have been caused by instability of the response lamp or by poor electrical contact between the lamp and its socket. Associated response scans were not used for processing of solar data.

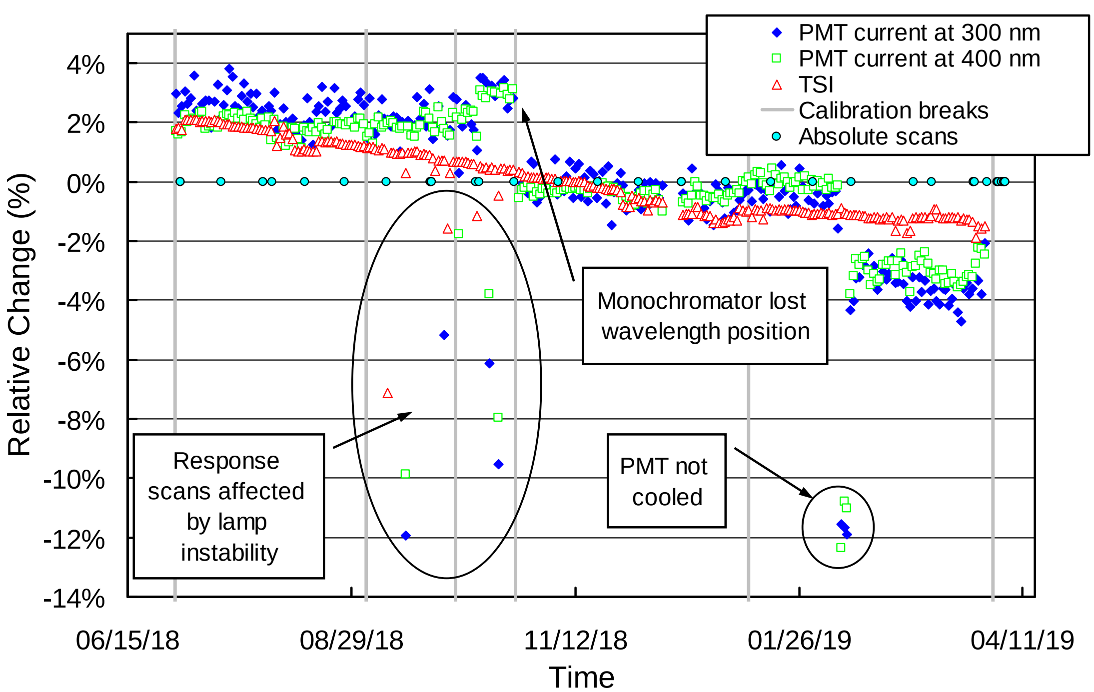

Figure 2. *Time-series of PMT current at 300 and 400 nm, and TSI signal. All data were extracted from measurements of the internal irradiance standard and are normalized to their average. Calibration break points (Table 1) and times of absolute scans are also indicated.*

The reporting period was divided into five calibration periods, labeled P1 – P5 (Table 1). Figure 3 shows ratios of the calibration functions applied during Periods P1 through P5 relative to the function of Period P1.

Table 1. Calibration periods for Palmer Volumes 28.

Period name	Period range	Number of absolute scans
P1	07/01/18 – 09/02/18	7
P2	09/03/18 – 10/02/18	5
P3	10/03/18 – 10/22/18	2
P4	10/23/18 – 01/08/19	7
P5	01/09/19 – 03/29/19	12

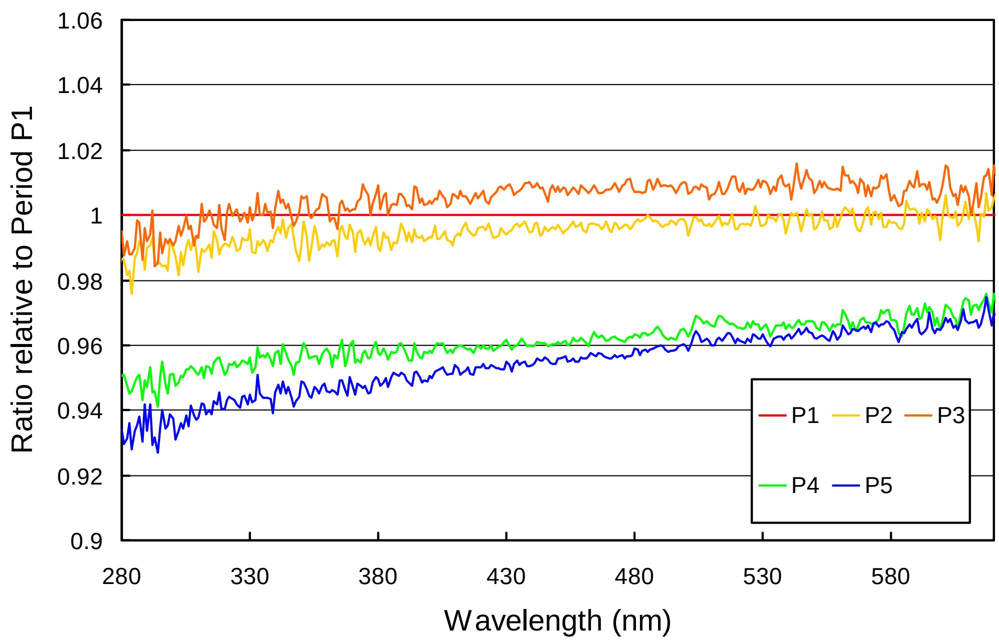

Figure 3. *Ratios of spectral irradiance assigned to the internal reference lamp for periods P1 – P5 relative to Period P1.*

The suitability of the selected calibration break points was checked by comparing calibrated SUV-100 measurements with GUV data. Figure 4 shows the ratio of GUV-511 data (340 nm channel) and final SUV-100 measurements, which were weighted with the spectral response function of this channel. The ratio is normalized and should ideally be one. There are virtually no step-changes at times of calibration breaks (green vertical lines), indicating that solar data of the SUV-100 have been appropriately corrected. GUV and SUV measurements typically agree to within ±5%. However, Figure 4 also shows a few short periods when the ratio is abnormally high (e.g., on 7/5/18 – 7/7/18, 7/30/18, 8/1/18, 8/19/18, and 11/5/18). On these days, snow was presumably covering the irradiance collector of the SUV-100 spectroradiometer for short periods. GUV measurements are less affected by snow because the instrument is heated to a higher temperature. Hence, the ratio of GUV and SUV measurements is high after heavy snowfall until the SUV collector is again free of snow. When disregarding periods affected by snow, GUV and SUV are consistent to within ±2.6% (±1σ). SUV measurements influenced by snow are part of the Version 0 and 2 datasets, and have been flagged in the Version 2 dataset.

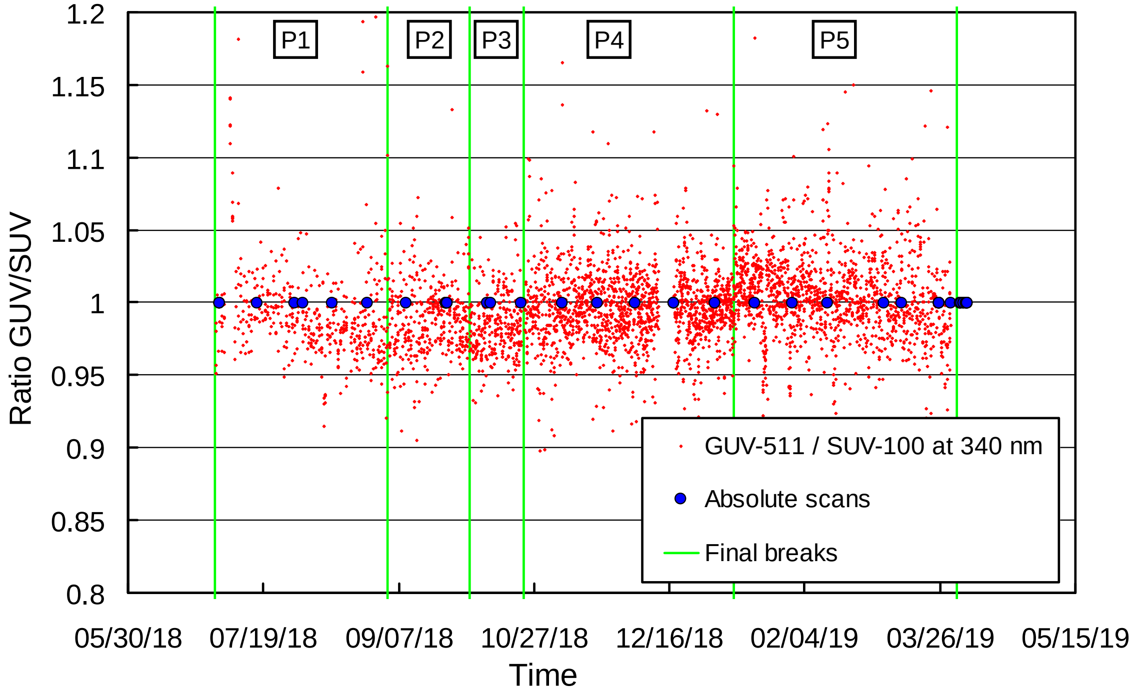

Figure 4. *Ratio of GUV-511 measurements at 340 nm with final SUV-100 measurements. The latter were weighted with the spectral response function of the GUV-511's 340 nm channel. Narrow clusters of vertical data points are caused by snow covering the SUV-100 collector.*

2.3. Wavelength Calibration

Wavelength stability of the system was monitored with the internal mercury lamp. Information from the daily wavelength scans was used to homogenize the data set by correcting day-to-day fluctuations in the wavelength offset. The wavelength-dependent bias of this homogenized dataset and the correct wavelength scale was determined with the Version 2 Fraunhofer-line correlation method (Bernhard et al., 2004). Figure 5 shows the correction function calculated with this algorithm. Figure 6 indicates the wavelength accuracy of final Version 0 data for five wavelengths in the UV and visible by running the Version 2 Fraunhofer-line correlation method a second time. Shifts are typically smaller than ±0.06 nm. (The standard deviations for wavelengths between 305 and 400 nm are 0.028 nm on average). The wavelength accuracy was further improved as part of the production of Version 2 data. Figure 7 shows the wavelength accuracy of Version 2 data. The standard deviations for wavelengths between 305 and 400 nm decreased to 0.025 nm.

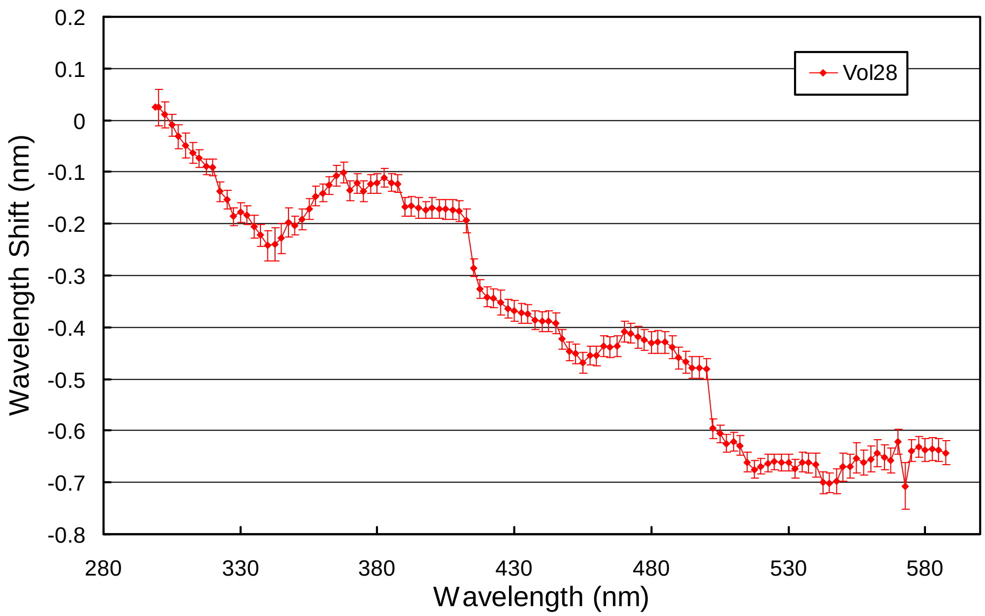

Figure 5. *Monochromator mapping function. Error bars indicate 1-σ variation.*

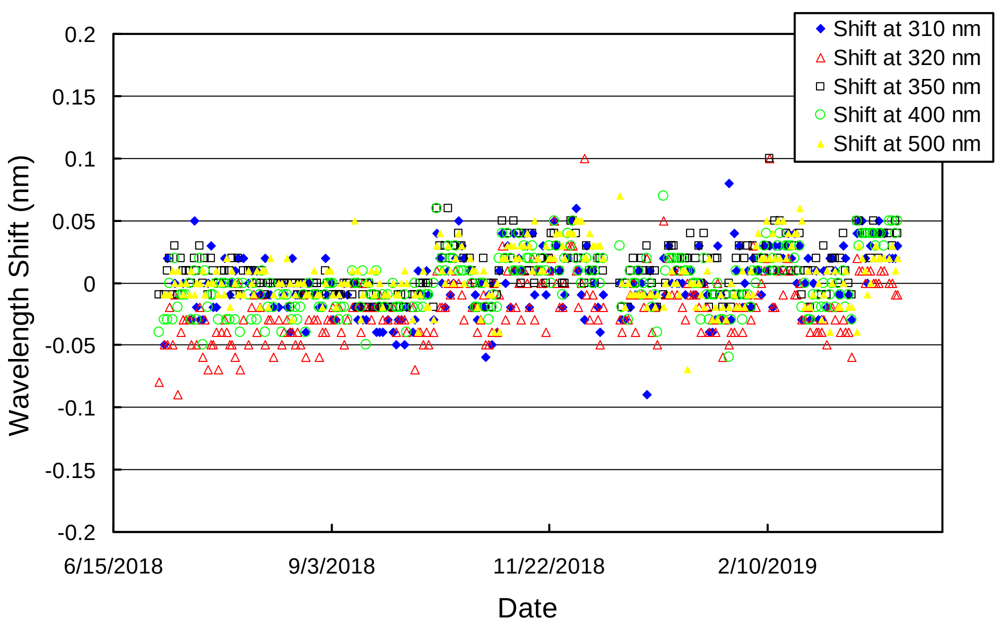

Figure 6. *Wavelength accuracy check of the final Version 0 data at five wavelengths by means of Fraunhofer-line correlation. Noontime measurements from every day of the year have been evaluated.*

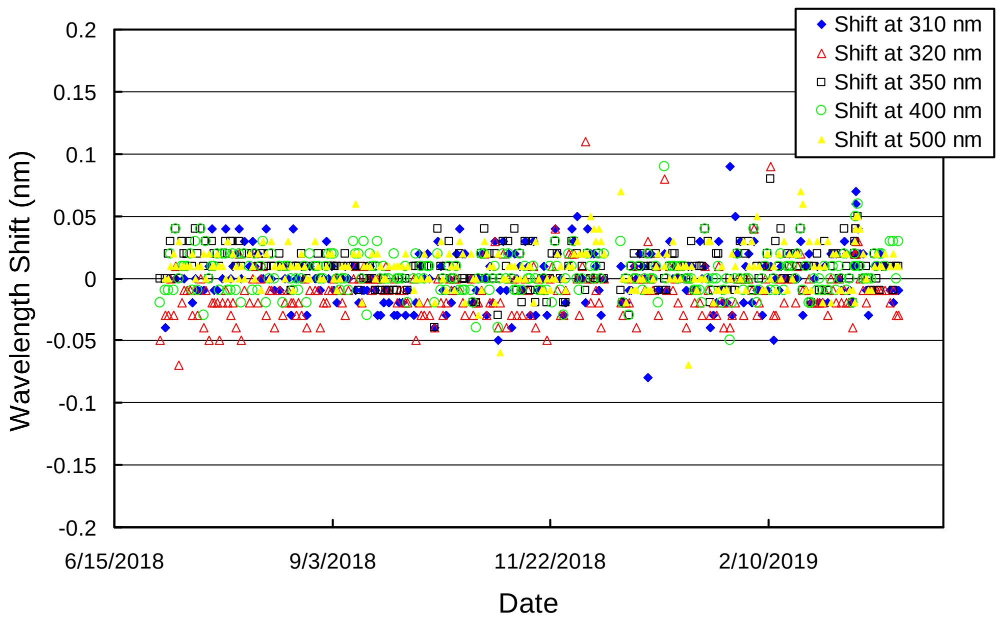

Figure 7. *Same as Figure 6 but for Version 2 data.*

2.4. Missing data

Table 2 provides a list of days that have substantial data gaps, and indicates their causes.

Table 2. Days with substantial data gaps.

Date	Reason
10/23/18	Large monochromator wavelength offset
12/12/18 – 12/17/18	Large monochromator wavelength offset

References

Bernhard, G., C. R. Booth, and J. C. Ehramjian. (2004). Version 2 data of the National Science Foundation's Ultraviolet Radiation Monitoring Network: South Pole, J. Geophys. Res., 109, D21207, doi:10.1029/2004JD004937.